Radio astronomy and interferometry

Silja Pohjolainen

Second solar lecture 2015

Nobeyama Radioheliograph (NoRH) antennas, Japan
Observing frequencies 17 and 34 GHz

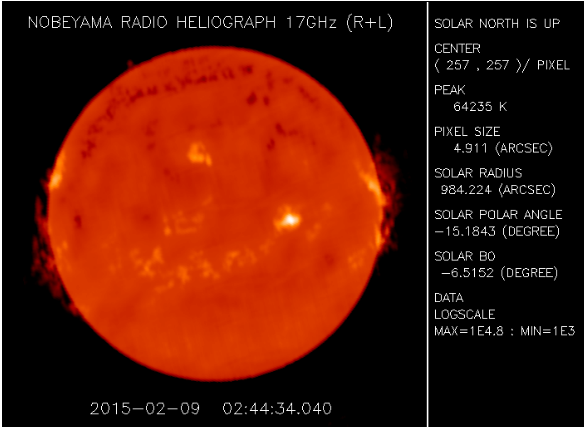
NOBEYAMA RADIO HELIOGRAPH 17GHz (R+L)
2015–02–09 02:44:34.040
SOLAR NORTH IS UP
CENTER
(257 , 257)/ PIXEL
PEAK
64235 K
PIXEL SIZE
4.911 (ARCSEC)
SOLAR RADIUS
984.224 (ARCSEC)
SOLAR POLAR ANGLE
–15.1843 (DEGREE)
SOLAR B0
–6.5152 (DEGREE)
DATA
LOGSCALE
MAX=1E4.8 : MIN=1E3

The Nançay Radioheliograph

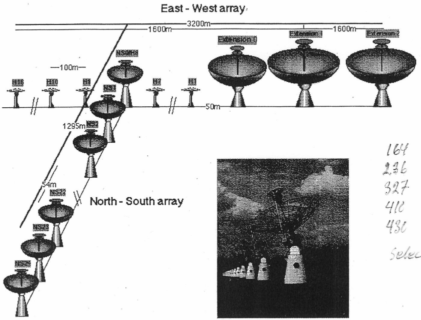

164 MHz
236
327
410
432
Selected

Arrays	Number of antennas	Minimum baseline	Maximum baseline	Beamwidth (150 MHz) [arcmin]	Beamwidth (450 MHz) [arcmin]
East-west	19	50.0 m	3200 m	1.3	0.42
North-south	24	54.3 m	1248 m	3.2-8.0 (1)	1.2-2.6 (1)

Time resolution: two 2D images/second at each frequency, 1996 →
ten 1D images/second/array at each frequency

Measurement of circular polarization (Stokes par. V)

Dynamic range: > 45 dB

Observing time: 8:30 to 15:30 UT

(1) during summer and winter months, respectively

Nancay Radioheliograph (NRH) antennas, France

Note the sufficient antenna surface when observing at low frequencies

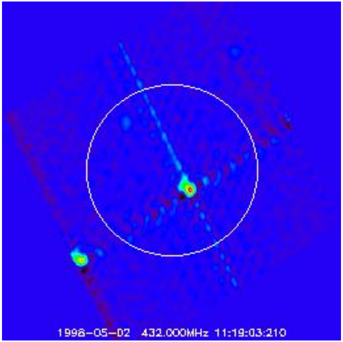

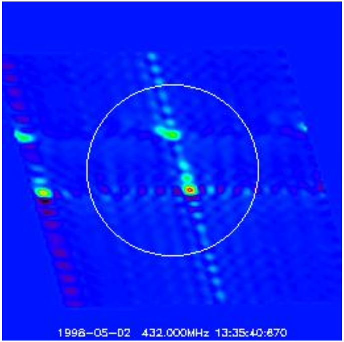

Interferometric patterns can still be visible after cleaning the images

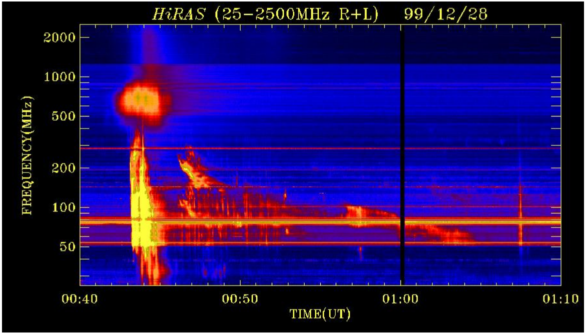

Hiraiso Radio Spectrograph (HiRAS) consists of three antennas, of which receiving frequencies are 25-70, 70-500, 500-2500 MHz

Ground-based observations are cut near 25 MHz due to Earth's ionosphere

Radio dynamic spectra from ground

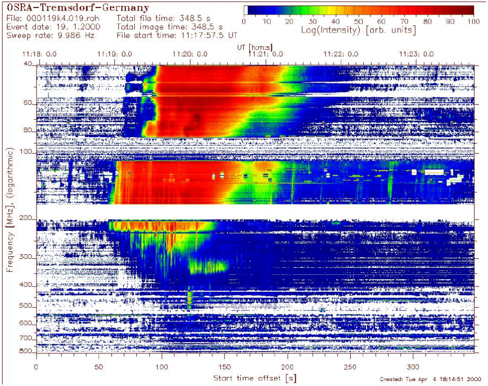

In dense-populated regions interference from TV-stations, radars, mobile phones, etc. can be strong

Bad bands are often removed from the spectral plots

Radio dynamic spectra from space

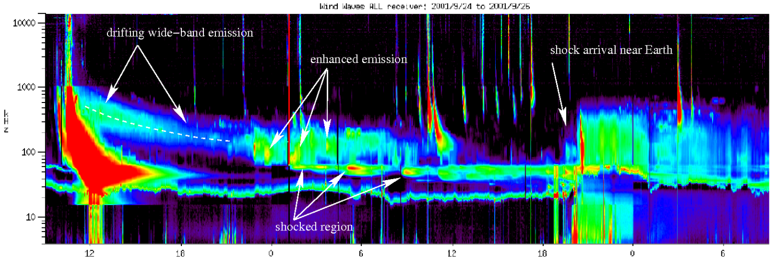

Wind WAVES

RAD2: 14–1 MHz, RAD 1: 1 MHz–20 kHz, TNR: 256–4 kHz

Plasma level near Earth is 20–40 kHz

Auroral kilometric radiation (AKR) creates additional 'noise'

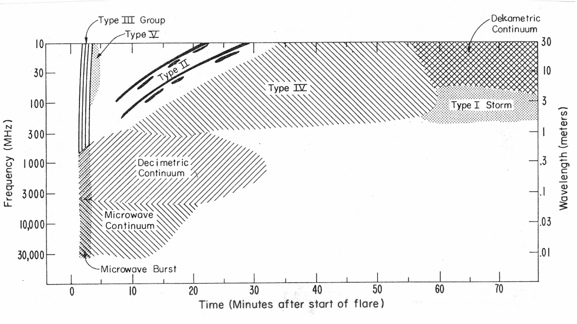

Radio continuum emission is typically observed at frequencies higher than ∼1–2 GHz ('microwave continuum')

Bremsstrahlung (free-free continuum emission)

- **Thermal bremsstrahlung**
- **Nonthermal bremsstrahlung**

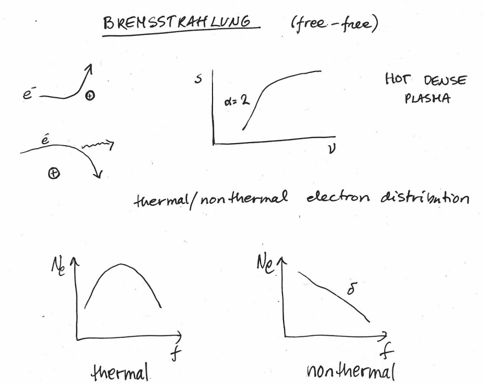

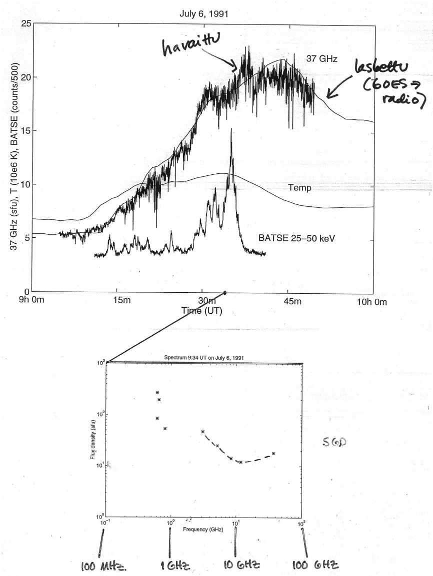

Gradual solar event:
observed radio flux and calculated flux from GOES X-rays

Gyroemission

The gyrofrequency ω_B for a particle with a charge q, mass m, and Lorentz factor γ, gyrating in a magnetic field B, pitch angle ψ being the angle between the B vector and the velocity vector, is in Gaussian units (Lang, 1980)

$$\omega_B = \frac{qB}{\gamma\, m\, c} \sin\psi$$

The gyrofrequency thus depends on the magnetic field strength B (in Gauss) and for non-relativistic electrons the gyrofrequency becomes

$$\nu_B = 2.8 \times 10^6 B \quad \text{(Hz)}$$

Gyroemission

Thermal or non-thermal particles gyrating in the magnetic field

- **Gyroresonance (cyclotron)**: non-relativistic ($\gamma = 1$) particles
- **Gyrosynchrotron**: mildly relativistic ($\gamma <$ 2-3) particles
- **Synchrotron**: relativistic particles

Gyroresonance (cyclotron) emission

$$\nu_B = 2.8 \times 10^6 B \quad \text{(Hz)}$$

- gyroresonance emission is concentrated at the fundamental frequency ($\omega = \Omega_e$) and at harmonics $s = \nu/\nu_B < 10$
- thermal electron distribution
- radiation is directed mainly along the magnetic field

Gyrosynchrotron emission

$$\nu_B = 2.8 \times 10^6 B \quad \text{(Hz)}$$

- gyrosynchrotron emission is strong at harmonic numbers $s = 10 < \nu/\nu_B < 100$
- both thermal and power-law electron distributions
- emission has a broad maximum perpendicular to the magnetic field

Synchrotron emission

$$\nu_B = 2.8 \times 10^6 B \quad \text{(Hz)}$$

- broad continuum at high harmonics, $s \sim (\gamma \sin\theta)^3$, i.e. near $\omega = \Omega_e \gamma^2 \sin\theta$
- power-law electron distributions only
- emission directed in the direction of instantaneous electron motion; peak of radiation perpendicular to the magnetic field

Numerical codes, see
http://hesperia.gsfc.nasa.gov/hessi/modelware.htm

RADIO EMISSION DIRECTIVITY

GYROSYNCHROTRON RADIATION:

- TRAPPING (FLARE LOOPS)

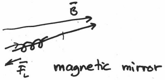

- BEAMING

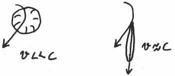

- VIEWING ANGLE

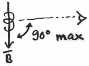

- RADIATED POWER $P \propto B^2$

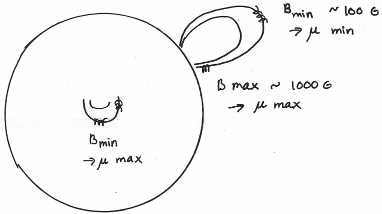

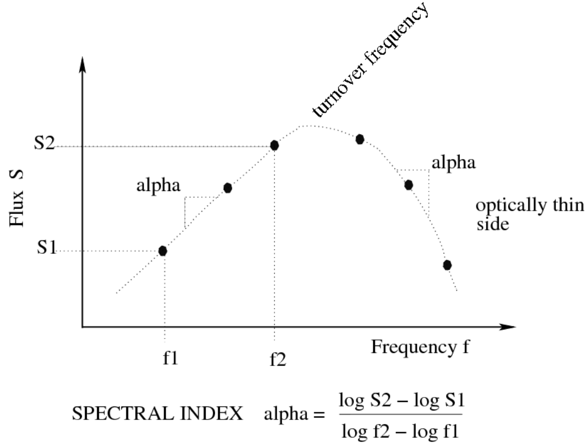

Particle energy diagnostics are always done using the OPTICALLY THIN (= high frequency) side of the spectrum!

GYROSYNCHROTRON RADIATION

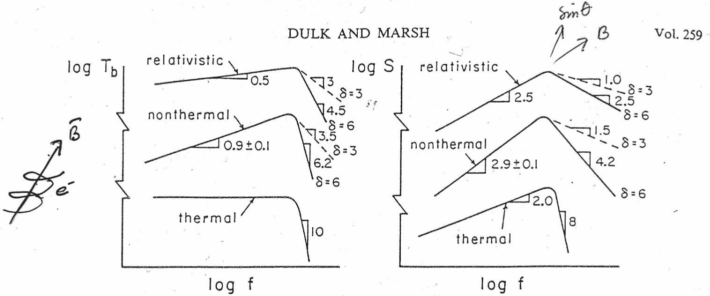

FIG. 2.—Shapes of brightness and flux spectra for thermal and nonthermal electron distributions. The shapes of the curves for relativistic power-law distributions were taken from Ginzburg and Syrovatskii (1965).

δ - electron power law

Astrophys. J. 259 (350 - 358)

Numerical codes for gyrosynchrotron (mildly relativistic)

Original calculations for gyrosynchrotron emission by Ramaty (1969), now widely used because computers are more powerful!.

For optically thin ($\tau \ll 1$, $\nu > \nu_{peak}$) sources the radio flux density reduces to

$$S_\nu = \frac{2k\nu^2}{c^2} \int \tau \, T_{ef} \; d\Omega = \eta \, L \, \Omega$$

$$\eta \approx 3.3 \times 10^{-24} \, 10^{-0.52\delta} \, (\sin\theta)^{-0.43+0.65\delta} \left(\frac{\nu}{\nu_B}\right)^{1.22-0.90\delta} BN,$$

$d\Omega$ = source solid angle, L = source length along the line of sight, N = particle density; valid for power-law indices $2 \leq \delta \leq 7$, viewing angles $\theta \geq 20^\circ$ and harmonic numbers $\nu/\nu_B \geq 10$.

Gyrosynchrotron emission: determining B

There is a way to determine B in the corona, using radio observations:

$$\nu_{peak} \approx 2.72 \times 10^3 \, 10^{0.27\delta} \, (\sin\theta)^{0.41+0.03\delta} \, (NL)^{0.32-0.03\delta} \, B^{0.68+0.03\delta}$$

But you need δ (from spectral hard X-ray observations), NL and θ (from soft X-ray, EUV, and/or radio imaging)...

These simplified expressions are by Dulk and Marsh (1982).

Numerical codes

Gyrosynchrotron emission: thermal electrons
For thermal electrons with a Maxwellian energy distribution Dulk and Marsh present a simplified expression suitable for semiquantitative analytical modelling for the optically thin spectral region.
Synchrotron emission: ultrarelativistic electrons
In the case of ultrarelativistic electrons the emission is very strongly beamed in the direction of the electron motion and collisions are rare.

(Not discussed here in detail by codes exist for all)

Examples of calculated flux density spectra

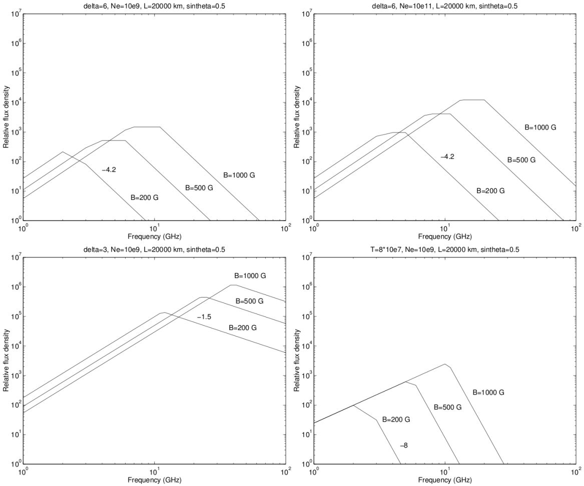

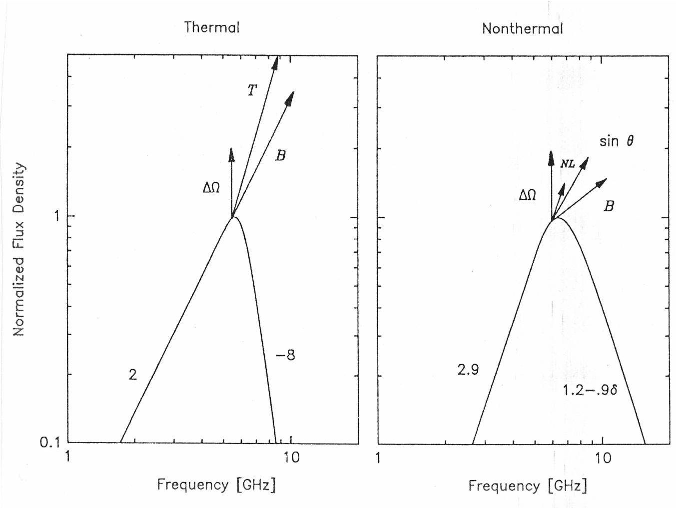

Parameters that can change the spectral shape

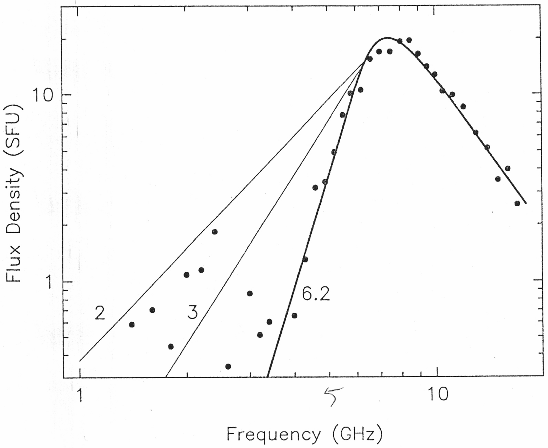

Fig. 8. Example of a spectrum with a steep low-frequency slope. The observed data points and the fit are shown together with the slopes expected from theory for a homogeneous source (about 2 for thermal and about 3 for nonthermal gyrosynchrotron emission).

Difficulties in spectral fitting

How to distinguish between bremsstrahlung and gyrosynchrotron emission?

- Thermal bremsstrahlung is only weakly polarized
- If plasma is isothermal and optically thick, polarization is zero
- Polarization in the optically thick side of gyrosynchrotron spectrum is extremely difficult to interprete
- On the optically thin side the degree of circular polarization in gyrosynchrotron emission is approximately 10...30%
- Polarization can be right (RCP) or left (LCP) handed and it can change during flare emission - depending on which end of the plasma loop electrons are gyrating
- Linear polarization has not been observed from the Sun (according to theory, it cannot propagate through the solar atmosphere)

Fixed frequency observations: gradual event

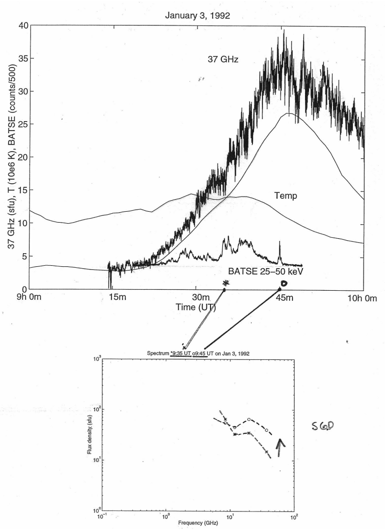

Spectral flattening: change from particle acceleration to heating

Fixed frequency observations: impulsive event

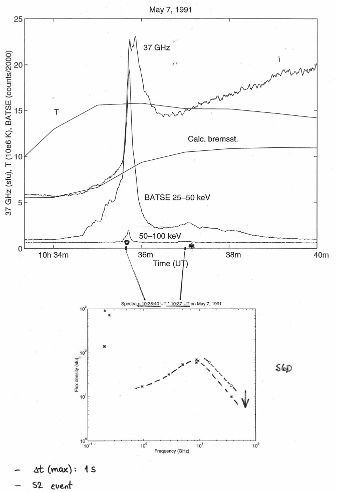

Spectral 'softening': decrease of energy in accelerated particles (opposite is spectral 'hardening' that may look the same as spectral 'flattening')

Masers

Maser = amplification of radio waves by stimulated emission of radiation

Solar case:
Electron cyclotron maser occurs when the resonance between electrons spiraling around a magnetic field and circularly polarised waves leads to growth of the waves

The condition of growth is certain form of **anisotropy** $\rightarrow$ loss cone anisotropy at loop footpoint

Occurs at ν_B and second harmonic

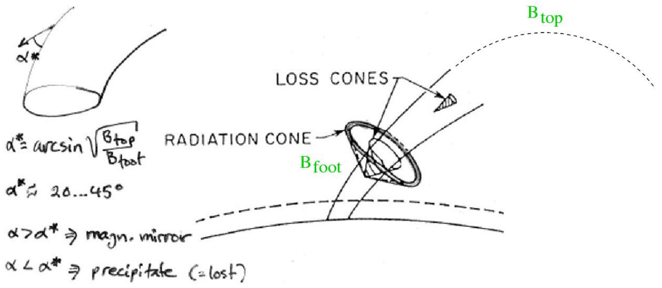

Loss-cone anisotropy: fast-propagating electrons hit and get absorbed; others reflect in the converging field

Electron-cyclotron masers

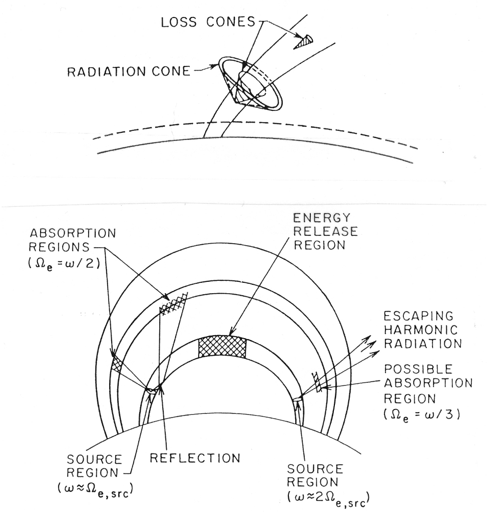

Figure 4 Schematic drawing of a sequence of magnetic flux tubes. At the top of a loop is a region where energy release is occurring. On the left is sketched a maser source region emitting at frequency $\omega = \Omega_e + \Delta$ at a location where the field strength is B_{sre}. The cone of radiation is shown, including a reflection of the portion directed toward higher field strength; this radiation is reabsorbed at locations where $B = B_{src}/2$. At the right is sketched a maser operating at $2\Omega_e + \Delta$, perhaps being reabsorbed where $B = 2B_{src}/3$.

Masers in action - radio spikes?

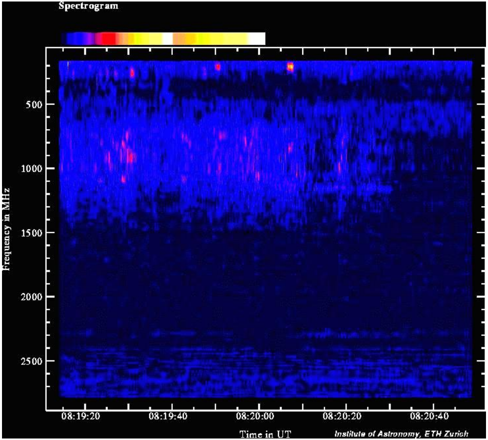

Spike characteristics: short duration, small bandwith, high brightness temperature (10^{15} K)

Absorption effects: Razin effect

The presence of a medium tends to suppress synchrotron and gyrosynchrotron radiation at low frequencies. The Razin frequency ν_R in a plasma with an electron density N_e is defined as

$$\nu_R = \frac{20N_e}{B} = \frac{2\nu_p^2}{3\nu_B}$$

For ultra-relativistic electrons the suppression occurs at $\nu \leq \nu_R$ and for mildly relativistic and non-relativistic electrons at harmonics $s = \nu/\nu_B \leq \nu_p^2/\nu_B^2$

(Melrose, 1985; Dulk, 1985).

Absorption effects

Gyrosynchrotron self-absorption
Absorption by the population of radiating electrons itself. The process reguires a strong magnetic field and a high column density of electrons

Free-free absorption
Collisional damping (free-free absorption) occurs when electrons begin to oscillate in resonance with the electric field and then collisions destroy the oscillation: the wave energy decreases and heats the plasma. Can happen when electromagnetic waves travel through cool dense structures in the solar atmosphere

Why is the radio flux rising at high frequencies in some events?
Possible answer: Absorption distorts the spectral shape

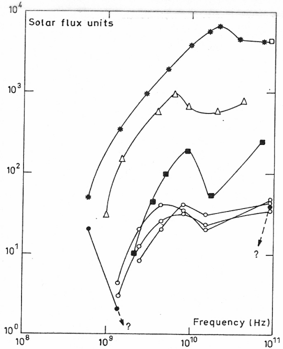

Fig. 3. Examples of solar burst spectra published in the literature, exhibiting a "flattening" towards mm-wavelengths or the superposition of a mm-wave spectral component. These results were obtained by the authors indicated is below. The measurements were taken with relatively poor time resolution and sensitivity. ∗ Croom (1970); □ Cogdell (1972); ○ Shimabukuro (1972); ● Shimabukuro (1970); ■ Akabane et al. (1973); △ Zirin and Tanaka (1973)

P. Kaufmann et al.: Synchrotron/inverse Compton solar burst emission

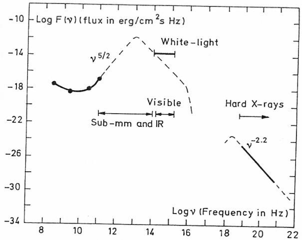

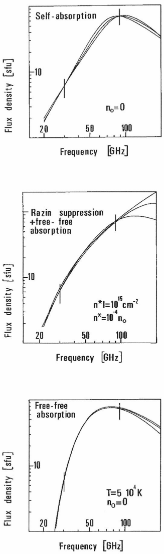

Fig. 4a–c. Gyrosynchrotron flux spectra computed for the mechanisms of absorption and suppression discussed in section 4 with the parameters of table 1 (1 sfu = $10^{-22}\,W\,m^{-2}\,Hz^{-1}$). Spectra are plotted for magnetic fields of 500 G, 1000 G and 2000 G (**a**), (**c**) and 250 G, 500 G and 1000 G (**b**) respectively. The vertical bars represent the observed flux densities at 30 and 90 GHz with an assumed error of 30%

outside the source of emission do not depend very much on the chosen parameters. This is different in the case where Razin suppression and free-free absorption inside the emissive source shape the spectrum: Most of the radiation above the spectral turnover frequency is then due to free-free emission, which is most intense at high electron densities and low temperatures.

In order to compare the numbers of energetic electrons in the microwave and the hard X-ray sources, we extrapolate the power-law spectrum (6) down to 10 keV and obtain the instantaneous number of nonthermal electrons at the peak of the microwave burst

$$N^*_\mu(10\,\text{keV}) = 10^{32} - 10^{34}\,.$$

The number $N^*_x(10\,\text{keV})$ of nonthermal electrons emitting hard X-rays through bremsstrahlung can be estimated from a power-law fit to the observed photon spectrum published by McClements and Brown (1986). With a spectral index of 3.2, Brown's (1971) Eq. 14, corrected by a factor π (Lin and Hudson, 1976), gives the instantaneous number

$$N^*_x(10\,\text{keV}) = \frac{3\,10^{45}}{n_0}\,,$$

where n_0 is the density in the hard X-ray source in cm^{-3}. For densities above $10^{11}\,cm^{-3}$, the instantaneous numbers of nonthermal electrons in the microwave and hard X-ray sources are thus in a fairly good agreement. The electron lifetime of 60 ms and the total duration of the event of 20 s inferred from Kaufmann et al. (1985) give a total number of $3\,10^{34}$ to $3\,10^{36}$ electrons accelerated during the event to more than 10 keV, which represent an energy of 10^{27} to 10^{29} erg.

The close temporal association of microwaves and hard X-rays down to the limits of temporal resolution of the hard X-ray spectrometer (Kaufmann et al., 1985) and the quantitative agreement between the *instantaneous* numbers of electrons suggest that the emissions come from a common source. As the hard X-rays are most efficiently emitted in a medium with high density of ambient electrons, this indicates that the plasma in the high-frequency source may be sufficiently dense, cool and magnetized to affect the microwave radiation by Razin suppression, free-free absorption and self-absorption. Each of these mechanisms can act with different efficiency at different points of a magnetic loop. It is to be emphasized, however, that both the derived parameters and the steep observed spectrum favour a very compact source with a small amount of inhomogeneity. The decimetric observations show that some of the accelerated particles are not confined in this source, but escape into structures with density below $10^{10}\,cm^{-3}$. The absence of significant microwave radiation below 30 GHz requires that the escaping electrons be highly anisotropic or that their number be very small.

As an alternative explanation of the observations, free-free absorption outside the flaring loop requires a cool and dense structure between the loop and the observer. Radio maps at 35 GHz (Hachenberg et al., 1978) show that small-scale structures exist which are not optically thin to millimetre waves. Filaments absorb microwave radiation down to millimetre wavelengths (Raoult et al., 1979) and were shown long time ago to shield occasionally microwave emitting loops (cf. Kundu, 1965). Furthermore, Mouradian et al. (1983) showed that during flares cold arches rise into the solar atmosphere with parameters ($T = 10^4 - 5\,10^5$ K, $n_0 \sim 10^{11}\,cm^{-3}$) that can account for the efficient absorption of microwaves in the millimetre band. In the

2800-2700 MHz SOLAR BURST PROFILES

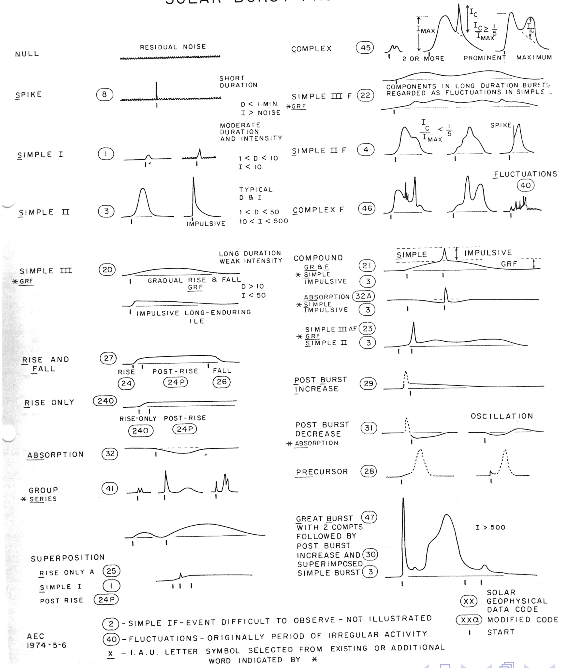

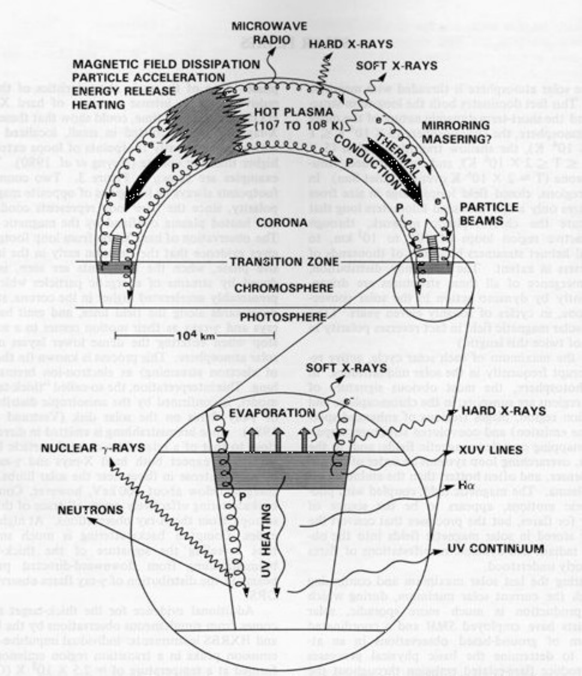

MICROWAVE
RADIO
HARD X-RAYS
SOFT X-RAYS
MAGNETIC FIELD DISSIPATION
PARTICLE ACCELERATION
ENERGY RELEASE
HEATING
HOT PLASMA
(10^7 TO 10^8 K)
MIRRORING
MASERING?
THERMAL
CONDUCTION
PARTICLE
BEAMS
CORONA
TRANSITION ZONE
CHROMOSPHERE
PHOTOSPHERE
10^4 km
SOFT X-RAYS
EVAPORATION
HARD X-RAYS
NUCLEAR γ-RAYS
XUV LINES
Hα
NEUTRONS
UV HEATING
UV CONTINUUM